Self–Configurable Actuator–Sensor Array for Active Vibration Suppression

Albert Schwinn and Hartmut Janocha
Laboratory for Process Automation (LPA)
Saarland University/Germany

This paper describes the use of distributed non–collocated piezoelectric patch actuators and sensors for active vibration control. The usually applied method for the design of an active vibration control is to describe first the modal behaviour of the structure and then to place the actuators and sensors according to an optimization criterion. This may lead to a non–optimal solution if the real system differs from the theoretical model and must be performed for every system to be considered. The new concept presented in this paper is to apply a number of piezoelectric ceramic patches onto a structure (e.g. during a production process), without necessarily knowing the structural behaviour in advance. This system is able to identify itself with the help of the ceramic patches and the specific functionality of a patch as an actuator, a sensor or as inactive, is determined according to a performance index. The major advantage of this smart structure is that it can perform an updated system identification if the system characteristics change and that it can choose a part of the ceramics as the best selection for actuators and sensors out of the whole quantity of ceramic patches. First experiments were carried out for the active vibration control of a beam with four piezoelectric patches bonded to it. Different actuator/sensor configurations for varying boundary conditions were studied, and the results are presented in this paper.

1 Introduction

The use of more and more lightweight structures for machines, vehicles etc. enforces the need for efficient structural vibration control, which can be achieved with active control methods. The use of induced strain elements, like piezoelectric ceramics or PVDF foils as actuators and/or sensors is described in several papers e.g. [7, 12, 13] to be effective for the design of smart structures. In order to achieve good results, an accurate model of the structure is needed. Mainly two approaches were made to build the models, namely continuous closed-formulations and discrete Finite Element Method solutions (FEM). Most of the continuous approaches [3, 4, 14] deal with simple structures, like beams and plates with basic boundary conditions. The ceramics are assumed to be perfectly bonded to the structure. This procedure prevents many practical implementations, where more complex structures could occur. The FEM based approaches [6, 9] can handle more sophisticated configurations and the results normally are accurate. But the models are in general very large and thus for the control a reduced model must be obtained. For both the continuous and the discrete approaches one has to know the physical properties of the structure in advance, in order to obtain a good model. This model may be in practice not always exact, because the system can change with time, or due to deviating boundary conditions. In order to optimize the control effect of the piezoelectric actuators, several authors developed optimization procedures for the size and the positions of the ceramic patches [2, 11]. This was accomplished for well–known structures under fixed boundary conditions.

In the present paper a different approach to active vibration suppression is presented. It is assumed that randomly placed ceramic patches were bonded onto a generally unknown structure. The frequency response between every patch will be determined in a first step by using some patches as actuators to excite the structure and others to measure the response, whereas each ceramic can serve as actuator or as sensor. An approximation of the measured response in the pole/residue form is made and with this a real parameter state–space model for the structure derived [1]. The applied control law for the controller is a Linear Quadratic Regulator (LQR) with a full state observer (Luenberger observer) [5, 8]. A performance index for the regulation is derived and used for the best selection of actuators and sensors out of all ceramics. Only a part of all patches can be used as actuators and sensors, because of limited computational and hardware capabilities. The results are verified with the real system and the effect of changed boundary conditions on the regulation performance and on the choice of actuators/sensors is studied in the last part of the paper.

2 Experimental setup

The experimental setup for verifying the applied method of vibration suppression consists of an aluminium beam which is clamped at both ends, according to Figure 1. The patches are glued onto

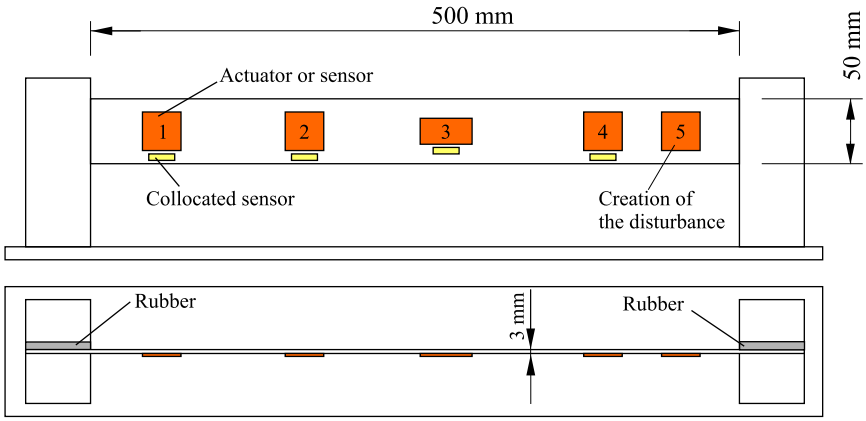

Fig. 1: Clamped beam with attached piezoelectric ceramics.
The rubber mounts are used for the non–rigid cases.

one side of the beam with EPOXY E-solder 3021. Patches 1–4 can be used for control and piezo number 5 will be used to create a disturbance. Next to each of the large patches, a small strip of piezoelectric material is glued onto the beam. They will only be used to analyze the frequency response of nearly collocated actuators and sensors and are not necessary for the proposed approach. Three different boundary conditions will be studied: rigid clamping of the beam on both sides, or rigid clamping on the right side and soft clamping with a rubber mount on the left side, and the other way round. The actuator and sensor dimensions are shown in Table 1. The test setup according to Figure 2 consists of 2nd–order Butterworth filters as reconstruction and antialiasing filters, the A/D–D/A converters, a PC for the signal processing, high voltage amplifiers ($\pm 100\,\mathrm{V}$) for the actuators and a switching array to select the best combination out of all ceramics as sensors and actuators.

3 Identification

In order to perform the experimental modal model identification, a bandlimited white noise signal is applied to one patch which serves in this case as actuator and the response is measured at the

Ceramic	Size (WxLxT) [mm^3]	Material	Collocated sensor	Size (WxLxT) [mm^3]	Material
1	29.7 x 29.7 x 1.0	PIC 151	1	2.5 x 20.0 x 1.0	PK11
2	29.7 x 29.7 x 1.0	PIC 151	2	2.5 x 20.0 x 1.0	PK11
3	20.0 x 40.0 x 1.5	PIC 151	3	2.5 x 20.0 x 1.0	PK11
4	29.7 x 29.7 x 1.0	PIC 151	4	2.5 x 20.0 x 1.0	PK11
5	29.7 x 29.7 x 1.0	PIC 151			

Table 1: Dimensions of the applied ceramics

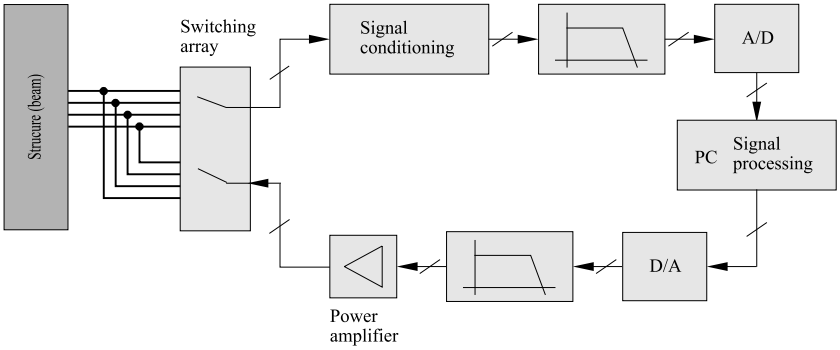

Fig. 2: Experimental setup

other patches, which serve as sensors. It can be assumed that the system is linear, time–invariant and reciprocal. Therefore only n measurements are necessary (n is the total number of large patches) in order to calculate n^2 frequency responses, including the collocated ones. The frequency responses are calculated using Welch's averaged periodogram method [10]. In order to compute the correct mechanical response of the beam, the antialiasing and the reconstruction filters must be considered.

$$H_{\mathrm{Mech}}(\mathrm{j}\omega) = \frac{H_{\mathrm{Measure}}(\mathrm{j}\omega)}{A * H_{\mathrm{Filter}}(\mathrm{j}\omega)} \tag{1}$$

A is the total gain of the amplifier and the A/D–D/A converters. An example for a calculated frequency response is shown in Figure 3. With this data, a model in the pole/residue (also called

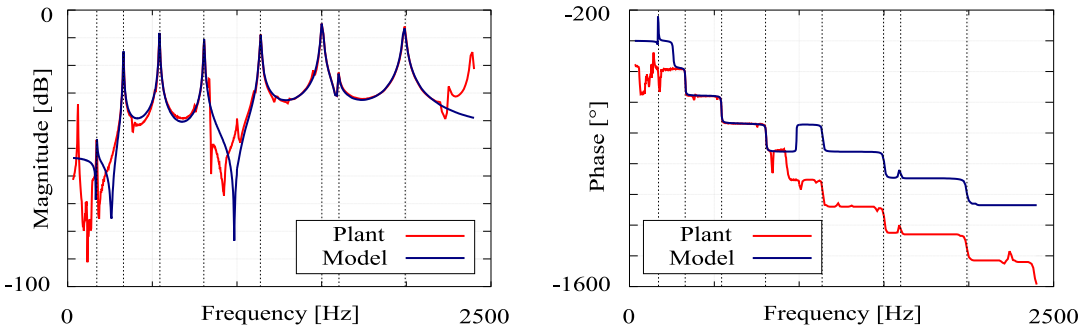

Fig. 3: Frequency response between ceramic 1 and ceramic 4

partial fraction expansion form) (2) is established

$$\mathbf{H}_{\text{Model}}(s) = \sum_{\text{j identified}} \left(\frac{\mathbf{R}_\text{j}}{s-\lambda_\text{j}} + \frac{\bar{\mathbf{R}}_\text{j}}{s-\bar{\lambda}_\text{j}}\right) + \mathbf{E}. \tag{2}$$

$\mathbf{R}_\text{j}$ and $\bar{\mathbf{R}}_\text{j}$ are the (complex conjugate) residues matrices, λ_j and $\bar{\lambda}_\text{j}$ are the (complex conjugate) poles and $\mathbf{E}$ is a correction matrix in order to account for neglected high–frequency modes. The poles of the identified model in Figure 3 are shown as dotted vertical lines. The model amplitude matches the measured data well, only the phase shows a difference above 900 Hz, which is due to a phase shift of 360°. The agreement between the measured data and the identified model is the result of a nonlinear least squares approximation of the measured data [1].
For control purposes one is interested in a linear state–space model of the form

$$\begin{aligned} \underline{\dot{x}}(t) &= \mathbf{A}\underline{x}(t) + \mathbf{B}\underline{u}(t) \\ \underline{y}(t) &= \mathbf{C}\underline{x}(t) + \mathbf{D}\underline{u}(t), \end{aligned} \tag{3}$$

where $\underline{x}(t)$ are the states, $\underline{u}(t)$ the actuator voltages and $\underline{y}(t)$ the sensor signals.

In order to obtain this model, one has to decompose the residues $\mathbf{R}_\text{j}$ into a dyad formed of a column vector $\underline{\psi}_\text{jc}$(the modal output), and a row vector $\underline{\psi}^\text{T}_\text{jb}$(the modal input). With this the following bloc–diagonal state–space form is given.

$$\begin{aligned} \begin{pmatrix} \underline{\dot{z}}(t) \\ \underline{\ddot{z}}(t) \end{pmatrix} &= \begin{pmatrix} \mathbf{0} & \mathbf{I} \\ -\mathbf{\Omega^2} & -\mathbf{\Gamma} \end{pmatrix} \begin{pmatrix} \underline{z}(t) \\ \underline{\dot{z}}(t) \end{pmatrix} + \begin{pmatrix} \mathbf{0} \\ \mathbf{\Psi}^\text{T}_\text{b} \end{pmatrix} \underline{u}(t) \\ \underline{y}(t) &= \begin{pmatrix} \mathbf{\Psi}_\text{c} & \mathbf{0} \end{pmatrix} \begin{pmatrix} \underline{z}(t) \\ \underline{\dot{z}}(t) \end{pmatrix}. \end{aligned} \tag{4}$$

$\mathbf{\Omega}^2 = \text{diag}(f^2_\text{modal})$ is the modal stiffness matrix, formed by the modal frequencies. $\mathbf{\Gamma}$ is the modal damping matrix. $\mathbf{\Psi}^\text{T}_\text{b}$ is the modal input matrix, formed by the modal input vectors and $\mathbf{\Psi}_\text{c}$ is the modal output matrix, composed of the modal output vectors. $\underline{z}(t)$ is the vector of modal displacements and $\mathbf{I}$ is the identity matrix. The final system to be considered for the control is the series of the identified mechanical system, the antialiasing and the reconstruction filters and is obtained through an extension of the state–space model (4).

4 Optimal control

The objective of structural control is to suppress the vibrations resulting from an external disturbance $\underline{f}(t)$. The state equation (3) can therefore be extended to

$$\begin{aligned} \underline{\dot{x}}(t) &= \mathbf{A}\underline{x}(t) + \mathbf{B}\underline{u}(t) + \mathbf{B}_\text{f}\underline{f}(t) \\ \underline{y}(t) &= \mathbf{C}\underline{x}(t) + \mathbf{D}\underline{u}(t). \end{aligned} \tag{5}$$

It is a major problem, that the overall displacement is not available for feedback. However, equation (5) shows that the control objective can be expressed as a problem of minimizing the state vector $\underline{x}(t)$ which is derived from the sensors. The feedback controller with the state observer is shown in Figure 4. The controller design can be divided into two steps. First, assuming the full state is available, an optimal state feedback gain matrix $\mathbf{K}$ is derived. In a second step, a state observer is built, which estimates the states from the sensed output voltages. The idea of the optimal control is to compute the control input

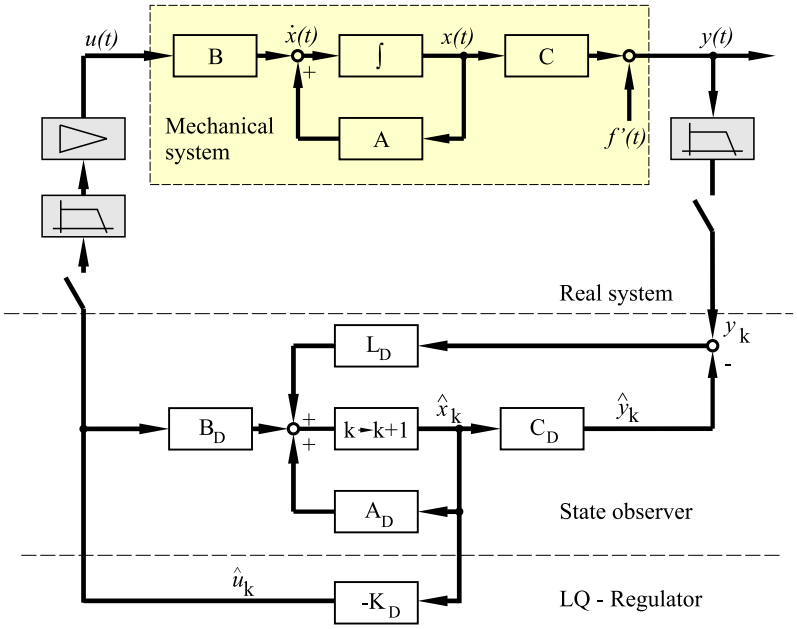

Fig. 4: Feedback controller with state observer

$$\underline{u}(t) = -\mathbf{K}\underline{x}(t), \tag{6}$$

such that the following quadratic cost functional is minimized

$$J = \int_0^\infty (\underline{x}^{\mathrm{T}}(t)\mathbf{Q}\underline{x}(t) + \underline{u}^{\mathrm{T}}(t)\mathbf{R}\underline{u}(t))\mathrm{d}t, \tag{7}$$

where $\mathbf{Q}$ and $\mathbf{R}$ are positive definite weighting matrices. The choice of $\mathbf{Q}$ and $\mathbf{R}$ is not unique and important for the controller design. It was found, that a good choice for the matrices is

$$\mathbf{Q} = \alpha_1 \mathbf{C}_{\mathrm{opt}}^{\mathrm{T}} \mathbf{C}_{\mathrm{opt}} + \alpha_2 \mathbf{I} \tag{8}$$

$$\mathbf{R} = \mathbf{I} \tag{9}$$

where $\mathbf{C}_{\mathrm{opt}}$ is the state–space matrix for the optimized sensor configuration, i.e. only those rows of the complete $\mathbf{C}$ matrix were kept which belong to the selected sensor ceramics. $\mathbf{I}$ is the identity matrix and α_1, α_2 are variables for the design of the controller. The minimization of the cost functional leads to the problem of solving an algebraic Riccati equation which can be performed using standard routines known from literature e.g. [5].
Since the state variables are not directly available for feedback, they have to be reconstructed by a state observer. The estimated state $\underline{\hat{x}}(t)$ is calculated from the control input $\underline{u}(t)$ and the output error vector $\underline{y}(t) - \underline{\hat{y}}(t)$ and the observer matrix $\mathbf{L}$, using the state–space model of the plant

$$\begin{aligned} \dot{\underline{\hat{x}}}(t) &= \mathbf{A}\underline{\hat{x}}(t) + \mathbf{B}\underline{u}(t) + \mathbf{L}(\underline{y}(t) - \underline{\hat{y}}(t)) \\ \underline{\hat{y}}(t) &= \mathbf{C}\underline{\hat{x}}(t) + \mathbf{D}\underline{u}(t). \end{aligned} \tag{10}$$

The poles of the observer must be located left of the set of control poles, to ensure that the observer algorithm is fast enough to track the states of the plant model. The observer poles were placed with a pole placement technique [10]. An example of the pole distribution is shown in Figure 5.

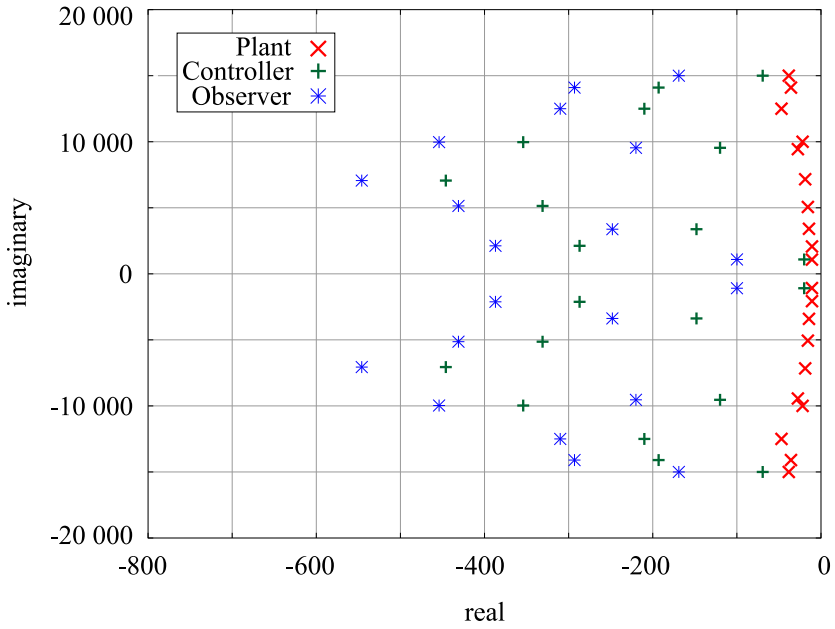

Fig. 5: Example of the pole map for the plant, the closed regulator loop and the observer. Actuator 4, sensor 1; boundary conditions: rigid clamping–rigid clamping.

It can be theoretically shown, that the ideal LQR has a guaranteed phase margin of 60°. In order to preserve this property as much as possible, the phase lag of the antialiasing and the reconstruction filter must be compensated through an extension of the state–space model of the beam. The whole system therefore to be considered is the series of the mechanical system and the two filters. This introduces four additional states because the filters are of second order.

5 Performance index

The ability of an actuator to suppress a mode and of a sensor to detect a mode depends on its positions relative to the nodes and antinodes of the mode. The afore calculated residues specify the magnitudes of the modes for the frequency responses. The residues of the frequency responses between two patches are therefore a measure for the use of one ceramic of this combination as an actuator and the other as a sensor. In order to penalize modes with small residues, which means that this combination cannot actuate or sense this mode, the performance index will be calculated as the product of the norm of the residues. This index must be specified for all possible combinations of actuators and sensors, which leads a the performance matrix with the elements

$$\mathbf{P}(m,p) = \prod_{\text{j identified}} \frac{|\mathbf{R}_\text{j}(m,p)|}{R_{\text{j,max}}} \qquad \begin{array}{lcl} m & : & 1\ldots\text{number of ceramics,} \\ p & : & 1\ldots\text{number of ceramics,} \\ j & : & 1\ldots\text{number of modes.} \end{array} \tag{11}$$

$$P_\text{Best} = \max\left(\mathbf{P}(m,p)\right) \tag{12}$$

Each residue value is normalized by its maximum value $R_{\text{j,max}}$ over all actuator–sensor combinations. The best choice for an actuator–sensor combination is the maximum value of all elements of $\mathbf{P}$. An example for the calculated performance matrix is given in Table 2. One can see that the combination

	Sensor			
Actuator	1	2	3	4
1	3.88e-7	5.42e-9	8.68e-8	9.14e-8
2	1.36e-8	6.83e-9	9.77e-10	2.99e-11
3	8.69e-8	1.42e-9	5.16e-9	7.25e-9
4	1.93e-7	3.04e-9	5.63e-9	4.05e-9

Table 2: Performance matrix for the boundary conditions 'rigid clamping on both ends'.

actuator 1, sensor 1 has the maximum performance. If the collocated cases were not considered than the combination actuator 4, sensor 1 is the best combination. The result is obvious for this simple case, because the patches 1 and 4 reside near both ends of the beam and can sense and actuate all modes in the frequency range up to 2 kHz, since there are no nodes in this area.

6 Results

The results are verified with the help of the small ceramic strips, in order to measure also the response at the location of the actuator. Figure 6 shows the power spectrum of the voltage for the choice of patch 4 as actuator and patch 1 as sensor. The boundary conditions are 'rigid clamping on both ends'. The spectrum can be significantly damped at the location of ceramic 1 and is slightly worse at location 4, which is due to the fact, that the disturbance acts near ceramic 4. According to Table

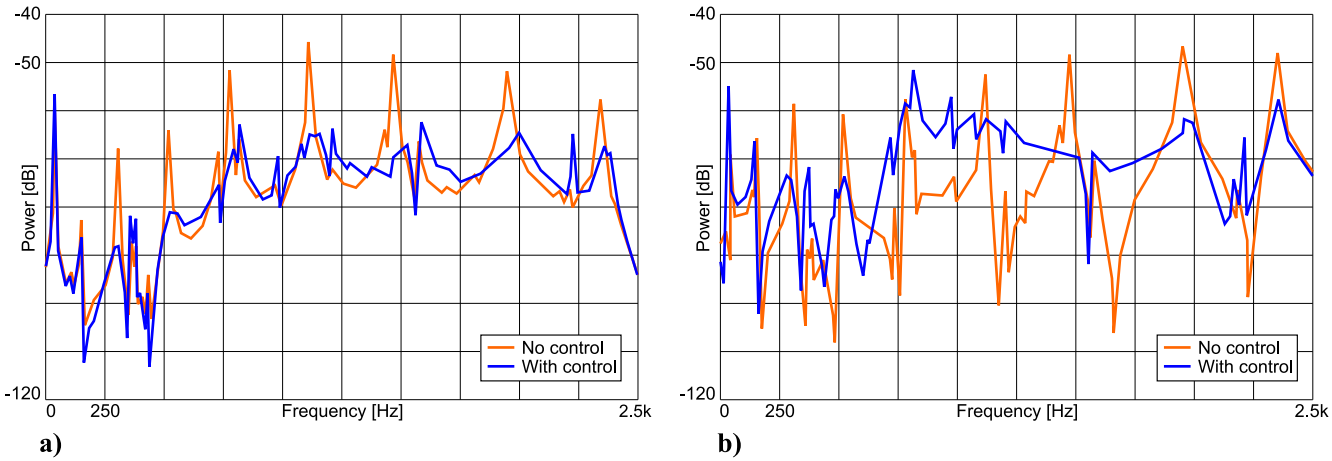

Fig. 6: Combination: actuator 4, sensor 1, boundary conditions: 'rigid clamping on both ends'. **a)** Power spectrum of the voltage at ceramic 1, **b)** Power spectrum of the voltage at ceramic 4.

2 the combination actuator 1/collocated sensor 1 is the best choice, although Figure 7 shows that the measured power spectrum is not as good as the combination actuator 4/sensor 1. This could be explained through local strain effects and was also observed for different experiments with nearly collocated actuators/sensors. It is therefore more efficient to use non–collocated actuators/sensors.

Table 3 shows the calculated acuator/sensor combinations for different boundary conditions, according to equation (11). Figure 8 shows the results for the boundary condition 'soft clamping–rigid clamping'. The results for the boundary conditions 'rigid clamping–soft clamping' are comparable and will be omitted here for brevity.

Boundary condition	Actuator	Sensor
Rigid–rigid	4	1
Soft–rigid	1	4
Rigid–soft	3	1

Table 3: Best actuator/sensor selections for different boundary conditions.

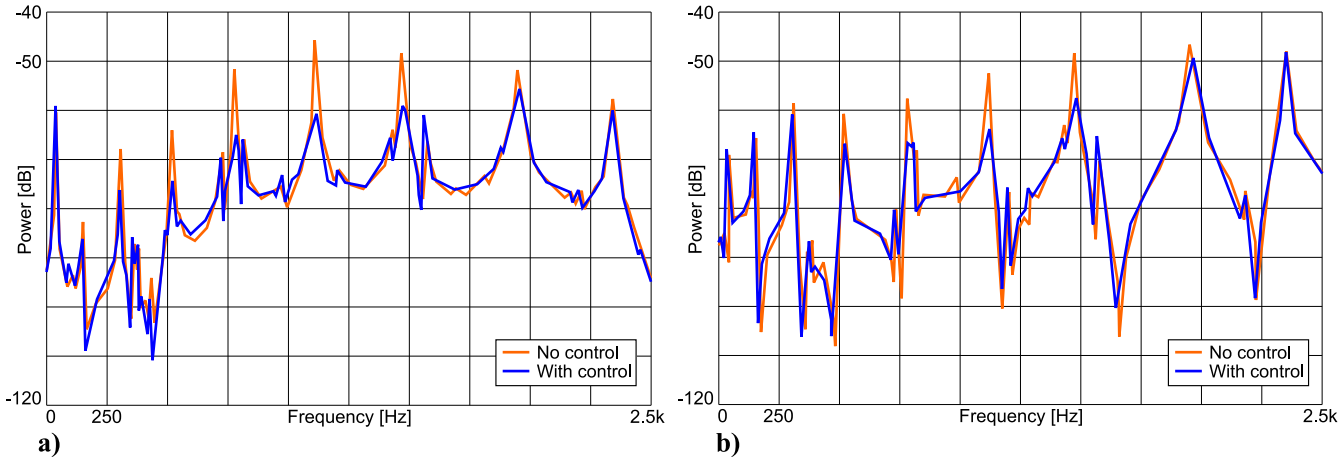

Fig. 7: Combination: actuator 1, sensor 1, boundary conditions 'rigid clamping on both ends'. **a)** Power spectrum of the voltage at ceramic 1, **b)** Power spectrum of the voltage at ceramic 4.

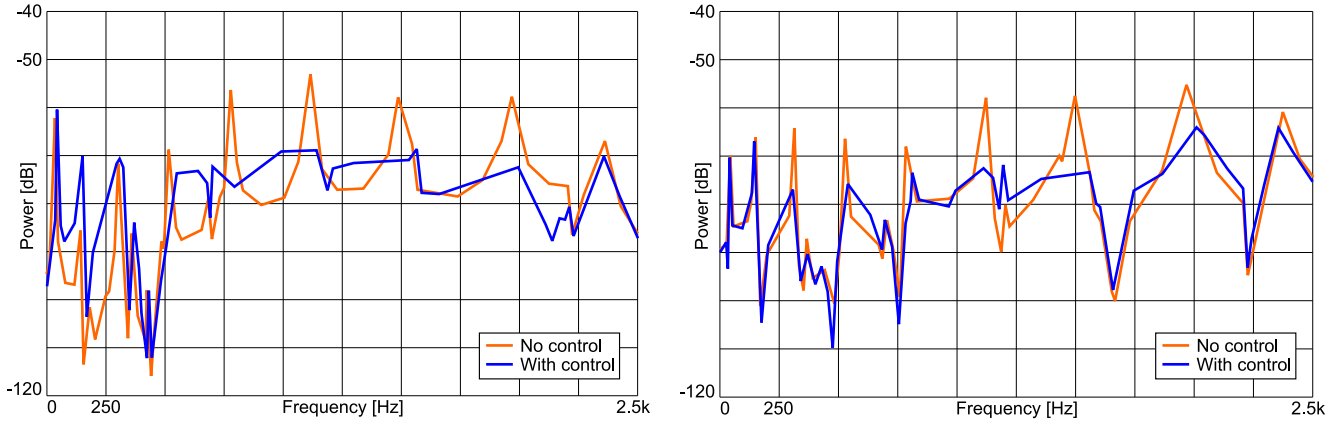

Fig. 8: Combination: actuator 1, sensor 4, boundary conditions 'soft clamping–rigid clamping'. **a)** Power spectrum of the voltage at ceramic 1, **b)** Power spectrum of the voltage at ceramic 4.

7 Summary

The vibration control experiments performed in this work demonstrate the efficiency of a self–configuring actuator–sensor array. It was shown that piezoelectric patches could be used to identify the modal behaviour of a unknown structure, although the positions of the ceramics may be randomly distributed over the surface. Depending of the identified modal characteristics of the structure different combinations of patches were found to be best used as actuators and sensors. It was shown that it may be necessary to change the selected choice, if the boundary conditions change. It is

thus possible to react to time varying conditions or to use the same type of structure in different applications, without the need of knowing the structural behaviour in advance.
Future work will concentrate on the implementation of an on–line identification technique for the modal characteristics, the use of more robust and self–tuning controllers and the extension of the performance index for the use of more than one actuator and sensor.

References

[1] Balmés, Etienne: *Structural Dynamics Toolbox for Matlab*. Scientific Software, 1998

[2] Concilio, A.; Lecce, L.; Ovallesco, A.: *Position and number optimization of actuators and sensors in an active noise control system by genetic algorithms*. **In:** ICEAS/AIAA Aeroacoustic Conference Aachen (1995), June, p. 633 – 642

[3] Dimitriadis, E.K.; Fuller, C.A.; Rogers, C.A.: *Piezoelectric actuators for distributed vibration excitation of thin plates*. **In:** Journal of Vibration and Acoustics 113 (1991), p. 100 – 107

[4] Falangas, Eric T.; Dworak, J.A.; Koshigoe, Shozo: *Controlling Plate Vibrations Using Piezoelectric Actuators*. **In:** IEEE Control Systems (1994), p. 34–41

[5] Föllinger, Otto: *Regelungstechnik*. Hüthig Verlag, 1990. – 6. Auflage

[6] Ha, S. K.; Chang, F.: *Finite Element Modeling of the Response of Laminated Composites with Distributed Piezoelectric Actuators*. **In:** Proc. of 31st AIAA/ASME/ASCE/AHS/ASC Structures , Structural Dynamics and Materials Conf. Long Beach (1990), p. 2323 – 2330

[7] Kim, S.J.; Jones, J.D.: *Optimal Design of Piezoactuators for Active Noise and Vibration Control*. **In:** AIAA Journal 29 (1991), December, Nr. 12, p. 2047 – 2053

[8] Lunze: *Regelungstechnik*. Springer Verlag, 1997. – Mehrgrößensysteme, Digitale Regelung

[9] Lim, Young-Hun; Varadan, Vasundara V.; Varadan, Vijay K.: *Closed–Loop Finite–Element Modeling of Active Structural Damping in the Frequency Domain*. **In:** Smart Materials and Structures 6 (1997), p. 161 – 168

[10] The Mathworks Inc.: *MATLAB Reference Guide*. 1998

[11] Main, John A.; Garcia, Ephrahim; Howard, Doug: *Optimal placement and sizing of paired piezoactuators in beams and plates*. **In:** Smart Materials and Structures 3 (1994), p. 373 – 381

[12] Preumont, André: *Active Structures for Vibration Suppressions and Precision Pointing*. **In:** Journal of Structural Control 2 (1995), June, Nr. 1, p. 49–63

[13] Rao, SS..; Sunar, M.: *Piezoelectricity and its Use in Disturbance Sensing and Control of Flexible Structures: A Survey*. **In:** Appl. Mech. Rev. 47, no 4 (1994), April, p. 113 – 123

[14] Yang, S. M.; Lee, Y. J.: *Interaction of structure vibration and piezoelectric actuation*. **In:** Smart Materials and Structures 3 (1994), p. 494–500